

Analytical flux density determination in the SPM slotless machine stator core

M. Bortolozzi ^{*}, N. Barbini ^{*}, M. Olivo [▼], A. Tassarolo [♦]

University of Trieste, Via A. Valerio 10, Trieste (Italy). E-mail: ^{*}mauro.bortolozzi@gmail.com, ^{*}nicola.barbini@phd.units.it, [▼]matteo.olivo@nidec-asi.it, [♦]atassarolo@units.it

Keywords: Slotless machine, analytical method, Laplace equation, magnetic field, stator core.

Abstract

Slotless machines equipped with surface permanent magnet (SPM) rotor are used in such applications where the torque ripple and the additional losses, due to the slotting effect, are critical issues. This kind of machine allows to find an accurate and analytical solution for the magnetic fields in every machine cross section domain. This paper derives an analytical expression for the magnetic field distribution inside the stator core of a SPM slotless machine during general load condition. The case of different rotor magnetization pattern is also considered. All the results are assessed with finite element analysis showing a very good accordance.

1 Introduction

In conventional PM machines, windings are fixed to a slotted stator core and retained usually with non-conductive wedges. This kind of arrangement is known to produce several parasitic phenomena like cogging torque or additional eddy currents losses in the magnets. There are several works (like [1]) in literature dealing with the air gap magnetic field evaluation in this kind of machines. In some applications, like wind power generation [2] or gas compression [3], it is necessary to overcome these issues in order to achieve very high efficiency and negligible torque ripples. One possible solution is to use the slotless stator structure. In this kind of electrical machines, the stator winding is completely distributed along the bore of an annular stator core and usually retained through a resin cast encapsulation.

Most of the literature dedicated to slotless machines focuses on the air-gap magnetic field evaluation for the performance prediction [4], [5], [6] and little or no attention is paid to the machine core. Actually, a previous work has focused on the magnetic field prediction inside the stator core, but limiting the scope of the treatment to the no load operation and to the use of a radially magnetized rotor [7]. The aim of this work is to extend the investigation proposed in [7] to find an analytical expression for the total magnetic field (due to both stator and rotor) in the stator core of a generic SPM slotless machine, equipped with a permanent magnet rotor with a generic magnetization pattern (parallel, radial, Halbach). The availability of an explicit analytical magnetic field

computation formula makes it possible to quickly estimate the iron core losses (using for example the Bertotti's formulation [8]-[11]). An analytical expression for the magnetic field (both radial and tangential components) in the iron core is possible through the solution of Poisson and Laplace differential equations in the machine domains of interest (core, air gap, magnets). In this paper, the explicit formulation for the total magnetic field is derived covering the case of SPM rotor topologies with different possible magnetization patterns: parallel, radial segmented and halbach magnetization. The accuracy of the proposed magnetic field expressions is then successfully assessed by comparison against Finite Element Analysis (FEA) for different numbers of poles and magnetization patterns.

2 Problem definition and model assumptions

Surface permanent magnet machines may be equipped with both slotted or slotless stator. The slotless structure allows to find a solution for the magnetic field distribution inside every machine domain solving the Laplace/Poisson differential equations ([4]). The rotor magnetization topologies addressed in this work are shown in Figure 1, where the arrows represent the magnetization direction inside the magnets region.

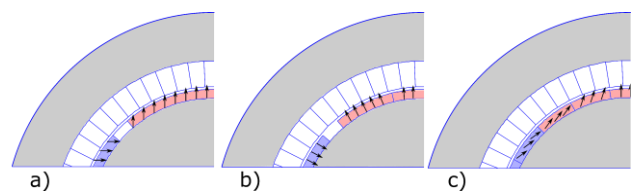


Figure 1: Rotor types considered in the analysis. a) Parallel magnetization, b) radial segmented magnetization, c) halbach array magnetization.

The rotor types being covered are: the parallel magnetization pattern Figure 1a; the segmented radial magnetization pattern Figure 1b, where each pole is composed by N_{seg} parallel magnetized magnets blocks; halbach magnetization pattern where each pole is composed again by N_{seg} parallel magnetized magnet blocks. This kind of rotor architectures are often used in permanent magnet machines ([12]).

Stator and rotor cores are assumed to have infinite magnetic permeability; the relative magnetic permeability of permanent magnets is supposed equal to unity.

End effects are disregarded, hence the vector potential is everywhere parallel to the rotational axis, so that its axial component is always considered as a scalar quantity.

3 Magnetic field evaluation in the slotless machine stator core

The aim of this section is the total magnetic field distribution evaluation in the stator core superimposing the contribution of the stator currents and the contribution of the magnets.

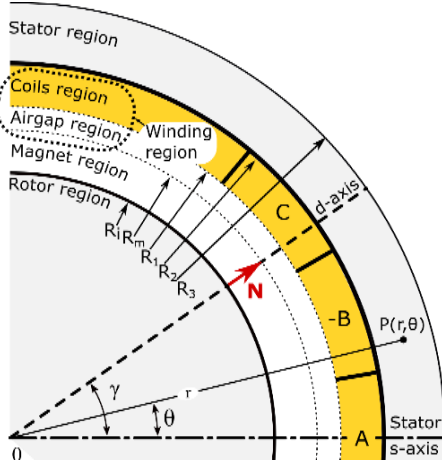


Figure 2: Characteristic dimensions of the machine cross-section. Stator s-axis and rotor d-axis are also represented.

3.1 Computation of the flux density in the stator core due to stator currents

In order to evaluate the stator currents contribution at the total magnetic field, it has been necessary to solve the Laplace equation (1) in the domain named as ‘‘Stator region’’ (Figure 2). This region is bounded with two circumferences whose radii are R_2 and R_3 for the inner and outer bound respectively. In a cylindrical coordinate system (r, θ, z) centered in the machine rotational axis, the vector potential (\mathbf{A}) in the stator region is governed by Laplace differential equation as follows:

$$\nabla^2 \mathbf{A} = \frac{1}{r} \frac{\partial}{\partial r} r \frac{\partial}{\partial r} A_z + \frac{1}{r^2} \frac{\partial^2}{\partial \theta^2} A_z = 0 \quad (1)$$

for $R_2 \leq r \leq R_3$

Using the Fourier expansion, this kind of partial differential equation it is known to have solutions like (2).

$$A_z(r, \theta, t) = \sum_{k_p=5p, 11p, \dots}^{\infty} \left(V_{k_p}^+ r^{k_p} + V_{k_p}^- r^{-k_p} \right) \cos(k_p \theta + \omega t) + \sum_{k_m=1p, 7p, \dots}^{\infty} \left(V_{k_m}^+ r^{k_m} + V_{k_m}^- r^{-k_m} \right) \cos(k_m \theta - \omega t) \quad (2)$$

Where V_n^+ and V_n^- are constants that have to be determined defined for k_p and k_m . Thanks to the relationship between the magnetic vector potential and the flux density in a planar

domain, the flux density produced by the coil currents in the stator region can be obtained as:

$$B_r^{st}(r, \theta) = \frac{1}{r} \frac{\partial A_z(r, \theta)}{\partial \theta} \quad (3)$$

$$B_\theta^{st}(r, \theta) = -\frac{\partial A_z(r, \theta)}{\partial r} \quad (4)$$

This said, it has been possible to determine the constants V_n^+ and V_n^- imposing the following boundary conditions:

$$B_r^{st}(R_3, \theta) = \frac{1}{r} \frac{\partial A_z(R_3, \theta)}{\partial \theta} = 0 \quad (5)$$

along Γ_4 in Figure 3

$$B_r^{st}(R_2, \theta) = \frac{1}{r} \frac{\partial A_z(R_2, \theta)}{\partial \theta} = BS_r^{b.c.}(\theta, t) \quad (6)$$

along Γ_3 in Figure 2

The boundary condition (5) is due to the fact that we want to impose the homogenous Dirichlet condition along the outer machine border. The second boundary condition (6) represents the radial magnetic field continuity between the winding region and the stator region Figure 2. The $BS_r^{b.c.}(\theta, t)$ function can be expressed using the results obtained in [4] as follows:

$$BS_r^{b.c.}(\theta, t) = \sum_{k_p} \frac{k_p}{r} w(r, k_p) \sin(k_p \theta + \omega t) + \sum_{k_m} \frac{k_m}{r} w(r, k_m) \sin(k_m \theta - \omega t) \quad (7)$$

Where the function $w(r, n)$ is the part that accounts for the dependency on r and can be expressed as follows for a generic n :

$$w(r, n) = \begin{cases} W_n^+ r^n + W_n^- r^{-n} - W_n^* r^2 & \text{if } n \neq 2 \\ \mu_0 J_2 \left[\frac{A + B(r)r^4}{4r^2(R_i^4 - R_2^4)} \right] & \text{if } n = 2 \end{cases} \quad (8)$$

In formula (8), coefficients A and $B(r)$ are given by:

$$A = R_1^4 R_2^4 - R_2^4 R_i^4 + 4R_2^4 R_i^4 \cdot \ln\left(\frac{R_1}{R_2}\right) \quad (9)$$

$$B(r) = R_1^4 - 2R_2^4 + R_i^4 + 4R_i^4 \cdot \ln\left(\frac{R_1}{r}\right) + 4R_2^4 \cdot \ln\left(\frac{r}{R_2}\right)$$

and coefficients J_n, W_n^+, W_n^- and W_n^* can be found in [4] at formulas (4), (15), (16) and (17).

As already said, in the Laplace equation solution (2), two constants must be determined. Substituting the equation (2) in the boundary conditions (3) and (4) two different equations are derived in the variables V_n^+ and V_n^- . Solving this liner system with two equations and two variables we can obtain:

$$V_n^- = \frac{R_2^n R_3^{2n} \cdot w(R_2, n)}{R_2^{2n} - R_3^{2n}} \quad (10)$$

$$V_n^+ = \frac{R_2^n \cdot w(R_2, n)}{R_3^{2n} - R_2^{2n}} \quad (11)$$

Thanks to these expressions, it is possible to express the magnetic field radial and tangential components due to only the stator currents as follows:

$$B_r^{st}(r, \theta, t) = - \sum_{\substack{k_p= \\ 5p, 11p, \dots}}^{\infty} k_p (V_n^+ r^{k_p-1} + V_n^- r^{-k_p-1}) \sin(k_p \theta + \omega t) - \sum_{\substack{k_m= \\ 1p, 7p, \dots}}^{\infty} k_m (V_n^+ r^{k_m-1} + V_n^- r^{-k_m-1}) \sin(k_m \theta - \omega t) \quad (12)$$

$$B_\theta^{st}(r, \theta, t) = - \sum_{\substack{k_p= \\ 5p, 11p, \dots}}^{\infty} k_p (V_n^+ r^{k_p-1} - V_n^- r^{-k_p-1}) \cos(k_p \theta + \omega t) - \sum_{\substack{k_m= \\ 1p, 7p, \dots}}^{\infty} k_m (V_n^+ r^{k_m-1} - V_n^- r^{-k_m-1}) \cos(k_m \theta - \omega t) \quad (13)$$

3.2 Computation of the flux density in the stator core due to the magnets

The aim of this section is to evaluate the magnetic field component in the stator core due to only the magnets mounted on the rotor. For this purpose, it is observed that, according to all the magnetization patterns taken into account (Figure 1), the rotor permanent magnets are arranged into uniformly-magnetized blocks. In order to simplify the computations, it has been necessary to consider a group of $2p$ magnet blocks displaced by π/p mechanical radians apart (Figure 3). As it can be deduced from Figure 3, regardless of the magnetization pattern, the magnetization vectors of magnet blocks displaced by π/p mechanical radians are shifted by 180° .

For the sake of simplicity, we shall also introduce a new angular coordinate φ measured from the axis of the first block of the group, so that a generic point p, in the rotor reference frame (Figure 3), will be identified with the couple of polar coordinates (r, φ) . This angular coordinate can be expressed as a function of θ as follows:

$$\varphi = \theta - \Theta \text{ where } \Theta = \frac{\omega t}{p} + \gamma \text{ so: } \varphi = \theta - \frac{\omega t}{p} - \gamma \quad (14)$$

where ω is the stator electric pulsation and γ is the angular shift between the stator s-axis and the rotor d-axis (Figure 2).

After the magnetic field computation for this ‘‘magnet group’’ the resultant flux density, for all the magnetization patterns, can be computed extending the result using a finite sum of elements.

In a similar way as already done in the previous section, the vector potential in the stator core due to a magnet block group only (Φ), can be expressed by the Laplace equation:

$$\nabla^2 \Phi = \frac{1}{r} \frac{\partial}{\partial r} r \frac{\partial}{\partial r} \Phi_z + \frac{1}{r^2} \frac{\partial^2}{\partial \varphi^2} \Phi_z = 0 \quad (15) \text{ for } R_2 \leq r \leq R_3$$

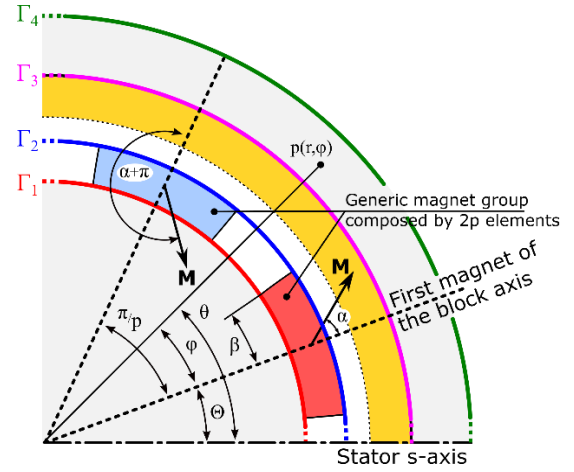


Figure 3: Two magnet blocks displaced by one pole pitch. The set of $2p$ magnet blocks displaced by π/p mechanical radians around the rotor surface is referred to as a ‘‘group’’ of magnet blocks.

It is known that this kind of partial derivative differential equation has solutions that can be expressed also as follows:

$$\Phi_z(r, \varphi, \alpha, \beta) = \sum_{n=1,3,5,\dots}^{\infty} (G_n^+(\alpha, \beta) r^{np} + G_n^-(\alpha, \beta) r^{-np}) \sin(np\varphi) + \sum_{n=1,3,5,\dots}^{\infty} (H_n^+(\alpha, \beta) r^{np} + H_n^-(\alpha, \beta) r^{-np}) \cos(np\varphi) \quad (16)$$

Where the parameters $G_n^+(\alpha, \beta)$, $G_n^-(\alpha, \beta)$, $H_n^+(\alpha, \beta)$ and $H_n^-(\alpha, \beta)$ are function of the magnet block semi opening angle β and function of the magnetization vector orientation α . These parameters can be determined by imposing the following boundary conditions:

$$B_r^{rot}(R_3, \varphi, \alpha, \beta) = \frac{1}{R_3} \frac{\partial \Phi_z(R_3, \varphi, \alpha, \beta)}{\partial \varphi} = 0 \quad (17)$$

along Γ_4 in Figure 3

$$B_r^{rot}(R_2, \varphi, \alpha, \beta) = \frac{1}{R_2} \frac{\partial \Phi_z(R_2, \varphi, \alpha, \beta)}{\partial \varphi} = BR_r^{b.c.}(\varphi, \alpha, \beta) \quad (18)$$

along Γ_3 in Figure 3

In the same way as the previous section, the condition (17) is due to the fact that we want to impose the nullity of the magnetic field radial component along the circumference Γ_4 . The other condition reported in (18) represents the continuity of the magnetic field radial component along the circumference Γ_3 . The $BR_r^{b.c.}(\theta, t)$ function can be expressed using the results obtained in [4] as follows:

$$BR_r^{b.c.}(\varphi, \alpha, \beta) = \sum_{n=1,3,5,\dots}^{\infty} (X_n^+(\alpha, \beta) r^{np} + X_n^-(\alpha, \beta) r^{-np}) \cos(np\varphi) - \sum_{n=1,3,5,\dots}^{\infty} (Y_n^+(\alpha, \beta) r^{np} + Y_n^-(\alpha, \beta) r^{-np}) \sin(np\varphi) \quad (19)$$

Where the coefficients $X_n^+(\alpha, \beta)$, $X_n^-(\alpha, \beta)$, $Y_n^+(\alpha, \beta)$ and $Y_n^-(\alpha, \beta)$ can be found in the paper [4] at formulas (91)-(101).

By substituting (16) into (17) and putting to zero the coefficients of $\sin(np\varphi)$ and $\cos(np\varphi)$, two linear equations are obtained in the unknowns variables $G_n^+(\alpha, \beta)$, $G_n^-(\alpha, \beta)$, $H_n^+(\alpha, \beta)$ and $H_n^-(\alpha, \beta)$. Substituting (16) and (19) into (18) and equalling the coefficients of $\sin(np\varphi)$ and $\cos(np\varphi)$ two more linear equations are obtained in the same variables. Now, solving this linear system we can obtain the desired variables and express them as follows:

$$\begin{aligned} G_n^+(\alpha, \beta) &= \frac{R_2^{2np} \cdot X_n^+(\alpha, \beta) + X_n^-(\alpha, \beta)}{R_2^{2np} - R_3^{2np}} \\ G_n^-(\alpha, \beta) &= \frac{R_3^{2np} (R_2^{2np} \cdot X_n^+(\alpha, \beta) + X_n^-(\alpha, \beta))}{R_3^{2np} - R_2^{2np}} \\ H_n^+(\alpha, \beta) &= \frac{R_2^{2np} \cdot Y_n^+(\alpha, \beta) + Y_n^-(\alpha, \beta)}{R_2^{2np} - R_3^{2np}} \\ H_n^-(\alpha, \beta) &= \frac{R_3^{2np} (R_2^{2np} \cdot Y_n^+(\alpha, \beta) + Y_n^-(\alpha, \beta))}{R_3^{2np} - R_2^{2np}} \end{aligned} \quad (20)$$

Thanks again to the relationship between the magnetic vector potential and the flux density vector it is possible to derive the final expression for the magnetic field (radial and tangential components) in the stator core due to only a group of $2p$ magnets:

$$B_r^{rot}(r, \theta, t, \alpha, \beta, \gamma) = \sum_{n=1,3,5...}^{\infty} (G_n^+(\alpha, \beta)r^{np-1} + G_n^-(\alpha, \beta)r^{-np-1}) \cos(np\theta - n\omega t - np\gamma) - \quad (21)$$

$$\sum_{n=1,3,5...}^{\infty} (H_n^+(\alpha, \beta)r^{np-1} + H_n^-(\alpha, \beta)r^{-np-1}) \sin(np\theta - n\omega t - np\gamma)$$

$$B_\theta^{rot}(r, \theta, t, \alpha, \beta, \gamma) = \sum_{n=1,3,5...}^{\infty} (G_n^+(\alpha, \beta)r^{np-1} + G_n^-(\alpha, \beta)r^{-np-1}) \sin(np\theta - n\omega t - np\gamma) - \quad (22)$$

$$\sum_{n=1,3,5...}^{\infty} (H_n^+(\alpha, \beta)r^{np-1} + H_n^-(\alpha, \beta)r^{-np-1}) \cos(np\theta - n\omega t - np\gamma)$$

where φ is substituted using formula (14).

3.3 Computation of the stator core total magnetic field for every rotor magnetization pattern

The total magnetic field distribution evaluation in the stator iron core it is possible superimposing the stator current contribution with the rotor magnet contribution. As already said in the first part of the paper, three different rotor magnetization patterns are considered for the total flux density evaluation. For this purpose, it is worth to notice that each magnetization pattern differs from the other only for the rotor contribution at the total magnetic field. The magnetic field component in the stator, due to the stator currents, is the same for each architecture. This said, it is possible to write the total

magnetic field for the SPM slotless machine with a parallel magnetized rotor as follows (Figure 1a):

$$B_r^{par}(r, \theta, t, \gamma) = B_r^{st}(r, \theta, t) + B_r^{rot}(r, \theta, t, \bar{\alpha}, \beta_{par}, \gamma) \quad (23)$$

$$B_\theta^{par}(r, \theta, t, \gamma) = B_\theta^{st}(r, \theta, t) + B_\theta^{rot}(r, \theta, t, \bar{\alpha}, \beta_{par}, \gamma) \quad (24)$$

where:

$$\beta_{par} = S_m \frac{\pi}{2p}, \quad \bar{\alpha} = 0 \quad (25)$$

The equation (25) means that, in a parallel magnetized rotor, each pole is composed by only one parallel magnetized block so there is no sum to perform. The magnet block magnetization direction is the same as the block symmetry axis (25). S_m is the permanent magnet span over the pole pitch ratio.

For the machine with the radial segmented SPM rotor (Figure 1b), the total flux density distribution in the stator core domain can be written as follows:

$$B_r^{seg}(r, \theta, t, \gamma) = B_r^{st}(r, \theta, t) + \sum_{b=0}^{N_{seg}-1} B_r^{rot}(r, \theta - \tau(2b+1), t, \bar{\alpha}, \beta_{seg}, \gamma) \quad (26)$$

$$B_\theta^{seg}(r, \theta, t, \gamma) = B_\theta^{st}(r, \theta, t) + \sum_{b=0}^{N_{seg}-1} B_\theta^{rot}(r, \theta - \tau_{seg}(2b+1), t, \bar{\alpha}, \beta_{seg}, \gamma) \quad (27)$$

where N_{seg} is the number of blocks composing a pole,

$$\tau_{seg} = S_m(\pi/2p) \text{ and } \beta_{seg} = S_m\pi/(2pN_{seg}) \quad (28)$$

Looking at equations (26) and (27), it is clear that a pole of the radial segmented rotor is composed by N_{seg} parallel magnetized blocks each with the magnetization direction correspondent to the block symmetry axis ($\bar{\alpha}=0$).

In the end, for the machine with the halbach array SPM rotor (Figure 1c), the total flux density distribution in the stator core domain can be expressed as:

$$B_r^{hal}(r, \theta, t, \gamma) = B_r^{st}(r, \theta, t) + \sum_{b=0}^{N_{seg}-1} B_r^{rot}(r, \theta - \tau_{hal}(2b+1), t, \overline{\alpha(b)}, \beta_{hal}, \gamma) \quad (29)$$

$$B_\theta^{hal}(r, \theta, t, \gamma) = B_\theta^{st}(r, \theta, t) + \sum_{b=0}^{N_{seg}-1} B_\theta^{rot}(r, \theta - \tau_{hal}(2b+1), t, \overline{\alpha(b)}, \beta_{hal}, \gamma) \quad (30)$$

where N_{seg} again the number of blocks per pole and:

$$\tau_{hal} = (\pi/2p), \quad \beta_{hal} = \pi/(2pN_{seg}) \quad (31)$$

Each block magnetization vector direction with respect its symmetry axis is:

$$\overline{\alpha(b)} = p[\beta(2b+1)] \quad (32)$$

3.4 Considerations about the stator core magnetic field evaluation

In some core loss evaluation methods [9]-[11], it is necessary to derive the trajectory described by the flux density fundamental harmonic vector in any point of the iron core. In general, such trajectory is an ellipse (as already shown in [7]). Again, the availability of an analytical expression for the radial and tangential flux density distributions in the stator core gives the ellipse trajectory of the magnetic field at any point of the stator core almost instantaneously (unlike finite element analysis). In Figure 4C the trajectory is shown for the flux density vector in points P1 and P2 for every machine architecture taken into account. All the derived equations underline the fact that the shape of the ellipse is strongly dependent only on the radial coordinate.

4 Finite elements validations

The final formulas for the flux density in the iron core are assessed by comparison with finite element results obtained on two different machines whose main data are reported in Table 1. The validation is performed considering each machine equipped with all the considered rotor architectures.

	Machine 1	Machine 2
R_i	47.5 mm	47.5 mm
R_m	57.5 mm	57.5 mm
R_1	58.5 mm	58.5 mm
R_2	62.0 mm	62.0 mm
R_3	90.0 mm	90.0 mm
H_c	850 kA/m	850 kA/m
μ_{mag}	1	1
S_m	0.95	0.95
p	2	3

Table 1: SPM machine data used for finite element validations

The comparison is made between the flux density computed analytically and with finite element along two different circumferences Γ_1 and Γ_2 Figure 5A and B. In the same figure is also represented the flux density trajectory in two different stator core points P_1 and P_2 Figure 5C). Formulas from (23) to (32) allow us to represent in the cartesian plane also the flux density fundamental vector trajectory (taking n , and k_m equal to 1 and excluding the part of the solutions (12) and (13) with k_p). This trajectory, as already said before, is an ellipse and is represented in the figure with the dashed line. Looking at the Figure 4 and 5, it is clear that the proposed method is in a very good agreement with the results derived from the finite element for both the polarities taken into account.

5 Conclusions

In conclusion, the paper addressed the solution of the magnetic field inside the stator core of a slotless permanent magnet machine, taking into account both the armature reaction and the permanent magnet contribution. The case of different SPM rotor magnetization patterns was also considered. Results have been compared with finite element calculations showing a very good accordance. The most straightforward use of the

formulations being presented is in the analytical computation of the core losses, including the eddy-current, hysteresis and other loss components. Further works will fully demonstrate this application and will compare the estimated iron core losses with measurements.

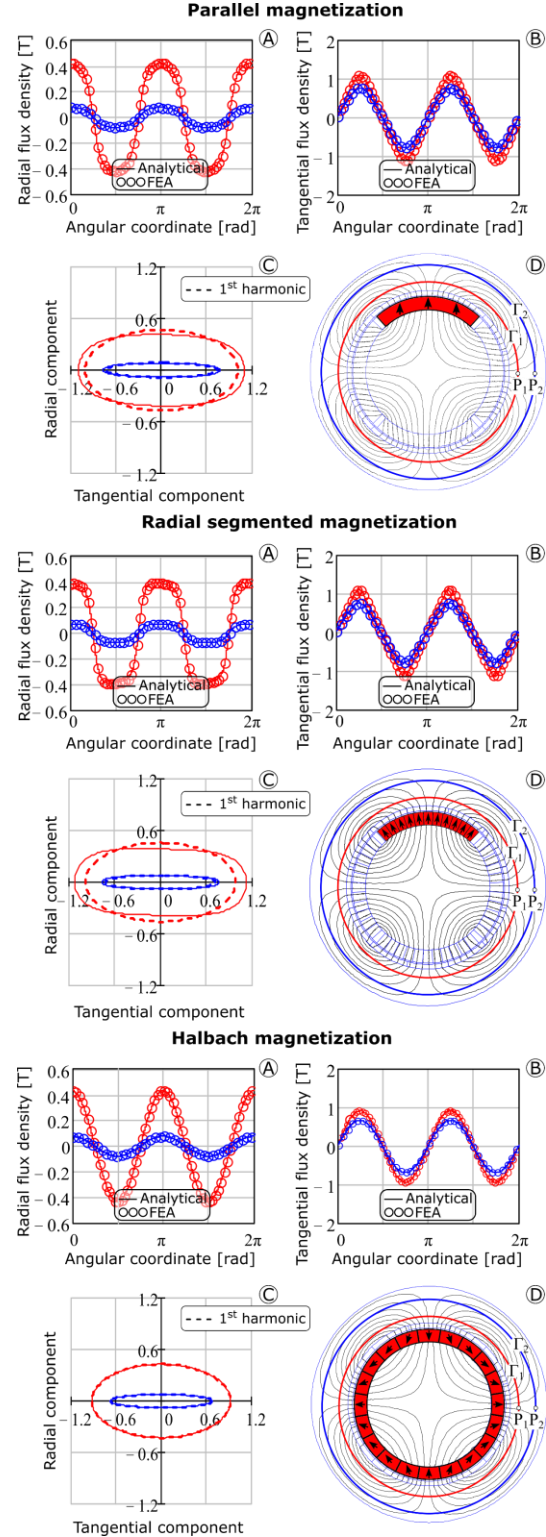


Figure 4 A and B: comparison of the flux density components along the circumferences Γ_1 and Γ_2 for all the rotor magnetization patterns; C: Flux density trajectory in P_1 and P_2 ; D: Machine under analysis cross section.

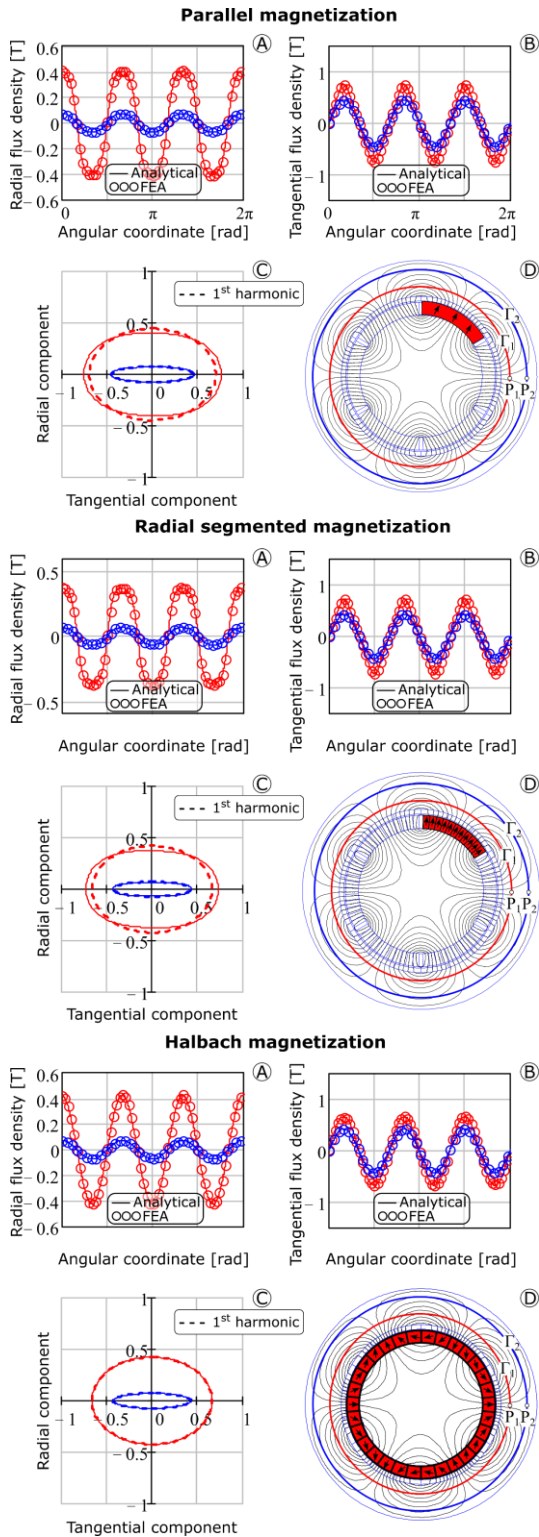


Figure 5: A and B: comparison of the flux density components along the circumferences Γ_1 and Γ_2 for all the rotor magnetization patterns; C: Flux density trajectory in P_1 and P_2 ; D: Machine under analysis cross section.

6 References

- [1] Z. Q. Zhu and D. Howe, "Instantaneous magnetic field distribution in permanent magnet brushless DC motors. IV. Magnetic field on load," in *IEEE Transactions on Magnetics*, vol. 29, no. 1, pp. 152-158, Jan. 1993.
- [2] A. Tassarolo, F. Luise, P. Raffin and V. Venuti, "Multi-objective design optimization of a surface permanent-magnet slotless alternator for small power wind generation," *2011 International Conference on Clean Electrical Power (ICCEP)*, Ischia, 2011, pp. 371-376.
- [3] F. Luise, F. Agnolet, S. Pieri, M. Scalabrin, M. Di Chiara, M. De Martin, "Design Optimization and Testing of High-Performance Motors: Evaluating a Compromise Between Quality Design Development and Production Costs of a Halbach-Array PM Slotless Motor," in *IEEE Industry Applications Magazine*, vol. 22, no. 6, pp. 19-32, Nov.-Dec. 2016.
- [4] A. Tassarolo, M. Bortolozzi and C. Bruzzese, "Explicit Torque and Back EMF Expressions for Slotless Surface Permanent Magnet Machines with Different Magnetization Patterns," in *IEEE Transactions on Magnetics*, vol. 52, no. 8, pp. 1-15, Aug. 2016.
- [5] Pfister, P.-D.; Perriard, Y.; "Slotless Permanent-Magnet Machines: General Analytical Magnetic Field Calculation," *Magnetics, IEEE Transactions on*, vol.47, no.6, pp.1739-1752, June 2011
- [6] Atallah, K.; Zi Qiang Zhu; Howe, D.; "Armature reaction field and winding inductances of slotless permanent-magnet brushless machines," *Magnetics, IEEE Transactions on*, vol.34, no.5, pp.3737- 3744, Sep 1998
- [7] L. Branz, M. Bortolozzi and A. Tassarolo, "Analytical calculation of the no-load flux density in the stator core of slotless SPM machines," *2013 International Conference-Workshop Compatibility And Power Electronics*, Ljubljana, 2013, pp. 244-249.
- [8] G. Bertotti, "General properties of power losses in soft ferromagnetic materials," in *IEEE Transactions on Magnetics*, vol. 24, no. 1, pp. 621-630, Jan 1988.
- [9] K. Yamazaki and N. Fukushima, "Iron-Loss Modeling for Rotating Machines: Comparison Between Bertotti's Three-Term Expression and 3-D Eddy-Current Analysis," in *IEEE Transactions on Magnetics*, vol. 46, no. 8, pp. 3121-3124, Aug. 2010.
- [10] J. V. Leite, M. V. Ferreira da Luz, N. Sadowski and P. A. da Silva, "Modelling Dynamic Losses Under Rotational Magnetic Flux," in *IEEE Transactions on Magnetics*, vol. 48, no. 2, pp. 895-898, Feb. 2012. doi: 10.1109/TMAG.2011.2173755
- [11] C. A. Hernandez-Aramburo, T. C. Green and A. C. Smith, "Estimating rotational iron losses in an induction machine," in *IEEE Transactions on Magnetics*, vol. 39, no. 6, pp. 3527-3533, Nov. 2003.
- [12] P. H. Mellor and R. Wrobel, "Optimization of a Multipolar Permanent-Magnet Rotor Comprising Two Arc Segments per Pole," in *IEEE Transactions on Industry Applications*, vol. 43, no. 4, pp. 942-951, July-aug. 2007.